Supporting Information

High Performance Ternary Organic Solar Cells Assisted by Red Fluorescent Materials Through Improved Emission Lifetime and Complementary Short Wavelength Light Absorption

Yingze Lei[a], Zhiyong Liu[a*] and Han Zhang[a]

[a]Institute of Physics and Electronic Information, Yunnan Normal University, Kunming 650500, China.

[*]Corresponding authors: (liuzhiyong@ynnu.edu.cn (Z.Y Liu))

4. Experimental details

4.1 Materials

PM6 and Y6 were purchased from Solarmer Materials Inc; DCJTB was purchased from Luminescence Technology Corp; Chloroform (CF) was purchased from Sigma-Aldrich Co. MoO_3 and Ag were purchased from Alfa Aesar Co. The photoactive solution with the blend of PM6, Y6 and DCJTB (the ratio of the PM6:Y6 is 1:1.3, PM6 content is 10 mg mL^{-1}, DCJTB content were varied according to measurement) was dissolved in CF and stirred overnight. The photoactive solution with the solvent additive of 1-chloronaphthalene (CN) (0.5%, v/v). The ZnO solution was synthesized by a sol-gel method [1, 2].

4.2 Device preparation and characteristics

Indium–tin-oxide (ITO) glasses were ultrasonicated at 30 °C in isopropyl alcohol, acetone and deionized water for 30 min. The ITO glasses were then dried by a stream of nitrogen and heated on the hot-stage. Firstly, spin-coating ZnO solution on the top of ITO glass (the speed is 3000 rpm and continue 1 min) and baked at 150 °C for 20 min in air (the thickness of ZnO thin films is 20 nm). The photoactive layer solution was spin-coated on the ZnO layer in a N_2-filled glove box to form the photoactive layer (the speed is 1800 rpm and continue 1 min), and the thermal annealing treatment (120 °C for 15 min, the nominal thickness of ~100 nm). The electron extraction layer of the MoO_3 layer and electrode of Ag films were evaporated under vacuum through a shadow mask to define the active area of the devices (2×2 mm^2). The OSC devices have an inverted configuration: ITO/ZnO/D18-Cl:Y6:DCJTB/MoO_3/Ag. All average

values with standard deviations were calculated from ten parallel devices. The current density versus voltage (*J–V*) characteristics of the OSCs were measured in a glove box with a computer-controlled Keithley 236 Source Measure Unit under illumination at 100 mW cm^{-2} using an AM1.5 G solar simulator. The external quantum efficiency (*EQE*) spectrum was measured with a Stanford Research Systems model SR830 DSP lock-in amplifier coupled to a WDG3 monochromator and a 500 W xenon lamp.

The space-charge-limited-current (SCLC) method was employed to investigate the charge carrier mobility. The charge carrier mobility was measured by the space charge limited current (SCLC) method, and the hole-only and electron-only devices had ITO/PEDOT:PSS/photoactive layer/Au and Al/photoactive layer/Al structures, respectively. The charge carrier mobilities were calculated using the following equation [3, 4]:

$$J = \frac{9}{8}\varepsilon_r\varepsilon_0\mu\frac{V^2}{d^3}$$

where *J* is the current density, μ is the charge carrier mobility, ε_0 (8.85×10^{-14} F/cm) and ε_r are the permittivity of free space and relative permittivity of the material (ε_r was assumed to be 3), respectively, and *V* is the SCLC effective voltage. The charge carrier mobility was calculated using the following equation [5]:

$$\mu = \mu_0 \exp[0.89\gamma\sqrt{\frac{V}{L}}]$$

where μ_0 is the charge mobility under zero electric field and γ is a constant. The Mott-Gurney equation can then be described by [6]:

$$J = \frac{9}{8}\varepsilon_r\varepsilon_0\mu_0\frac{V^2}{L^3}\exp[0.89\gamma\sqrt{\frac{V}{L}}]$$

In this case, the charge mobility were estimated using the following equation [6]:

$$\ln(\frac{JL^3}{V^2}) = 0.89\gamma\sqrt{\frac{V}{L}} + \ln(\frac{9}{8}\varepsilon_r\varepsilon_0\mu_0)$$

4.3 XRD Measurement

The angles at which the peak intensities occur are related to the inter-planar distances of the atomic structure of the photoactive layer and the crystallinity of the photoactive layer; these angles are related by Bragg's law [7]:

$$\lambda = 2d\sin\theta$$

where λ is the wavelength of the X-ray radiation used (0.154 nm), θ is the peak position half-angle, and *d* is the inter-planar distance.

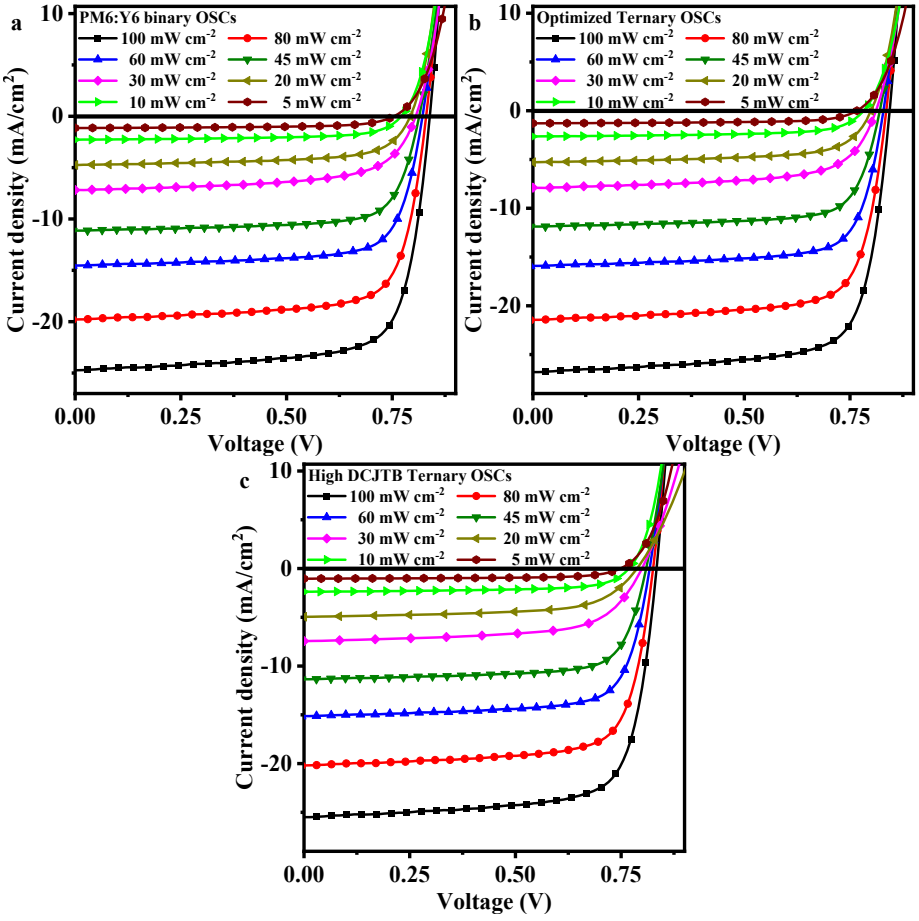

Figure S1. *J-V* characteristics of typical OSCs of PM6:Y6 based binary OSCs, optimized ternary OSCs and high DCJTB ternary OSCs under various light intensities ranging from 100 mW cm^{-2} to 5 mW cm^{-2} corresponding to Figure S1(a), S1(b) and S1(c), respectively.

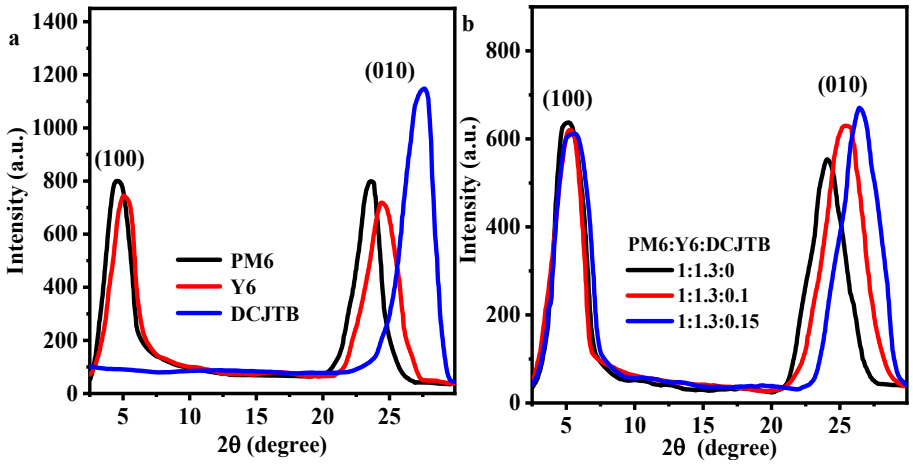

Figure S2. The XRD curve of neat films (PM6, Y6 and DCJTB) for (a) and three typical films (PM6:Y6 binary film, optimized ternary film and high DCJTB ternary film) for (b).

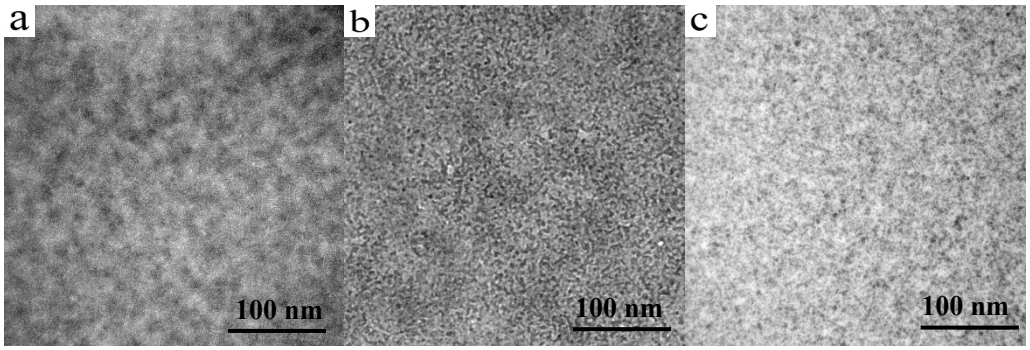

Figure S3. The TEM image of neat PM6, Y6 and DCJTB films.

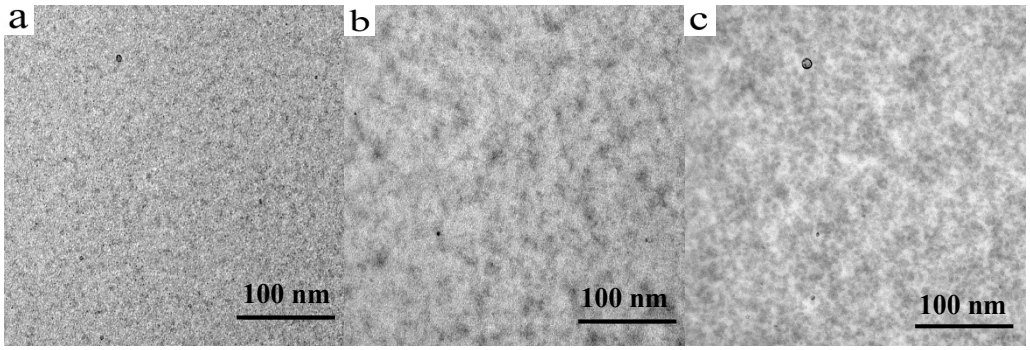

Figure S4. The TEM image of three typical films.

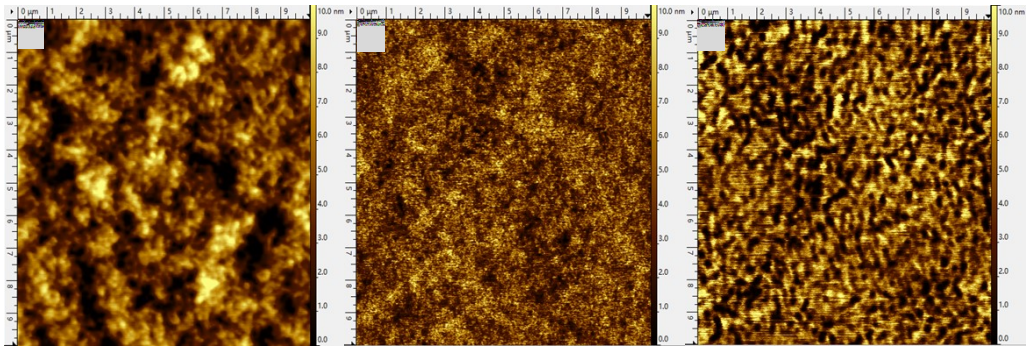

Figure S5. The AFM image of neat PM6, Y6 and DCJTB films.

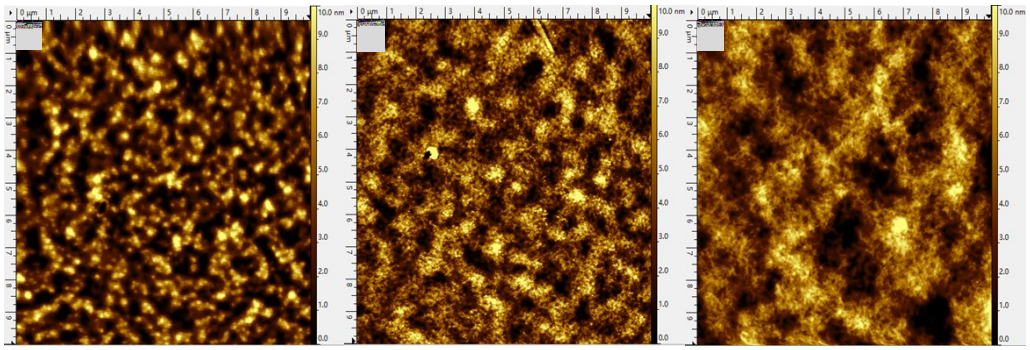

Figure S6. The AFM image of three typical films.

Reference:

1. W. Yu, L. Huang, D. Yang, P. Fu, L. Zhou, J. Zhang and C. Li, *Journal of Materials Chemistry A*, 2015, **3**, 10660-10665.
2. U. Galan, Y. Lin, G. J. Ehlert and H. A. Sodano, *Composites Science and Technology*, 2011, **71**, 946-954.
3. H.-W. Li, Z. Guan, Y. Cheng, T. Lui, Q. Yang, C.-S. Lee, S. Chen and S.-W. Tsang, *Advanced Electronic Materials*, 2016, **2**, 1600200.
4. V. Narasimhan, D. Jiang and S.-Y. Park, *Applied Energy*, 2016, **162**, 450-459.
5. Q. An, F. Zhang, Q. Sun, M. Zhang, J. Zhang, W. Tang, X. Yin and Z. Deng, *Nano Energy*, 2016, **26**, 180-191.
6. Q. An, F. Zhang, W. Gao, Q. Sun, M. Zhang, C. Yang and J. Zhang, *Nano Energy*, 2018, **45**, 177-183.
7. L. Zhao, S. Zhao, Z. Xu, Q. Yang, D. Huang and X. Xu, *Nanoscale*, 2015, **7**, 5537-5544.